02,10

Magnetic instabilities in the nanocomposite porous glass/Bi−Si alloy

© A.L. Pirozerskii[1], E.V. Charnaya[1], Kh.A. Abdulamonov[1], M.V. Likholetova[1], Yu.A. Kumzerov[2], A.V. Fokin[2]

[1] St. Petersburg State University,
St. Petersburg, Russia
[2] Ioffe Institute,
St. Petersburg, Russia

E-mail: e.charnaya@spbu.ru

Received November 29, 2024
Revised November 30, 2024
Accepted November 30, 2024

The paper presents studies of thermomagnetic instabilities in the nanocomposite porous glass/Bi−Sn alloy within a temperature range of superconductivity. Measurements of the temperature dependence of magnetization at a field of 10 G revealed the superconducting transition with temperature 4.2 K. The magnetization isotherms below the transition temperature corresponded to type II superconductivity with strong pinning. Incomplete jumps of magnetization were observed in the central part of the hysteresis loops at close values of external magnetic field. The hysteresis loops with magnetic instabilities were numerically modeled within the framework of the adiabatic approach modified taking into consideration the finite rate of temperature relaxation in the sample.

Keywords: superconductivity, magnetic instabilities, nanocomposite porous glass/Bi−Si alloy, magnetization isotherms.

DOI: 10.61011/PSS.2025.02.60670.326

1. Introduction

Magnetic instabilities in type II superconductors have been actively studied for more than 50 years due to their importance for practical applications of superconducting materials [1–3]. The occurrence of magnetic instabilities is caused by the redistribution of Abrikosov vortices existing in the mixed state of a type II superconductor under the influence of weak perturbations, for example, temperature fluctuations. Under the condition of equilibrium in an external field exceeding the lower critical field, a critical state is established in a superconductor as a result of self-organization, in which the currents associated with the spatial inhomogeneity of the magnetic field in the sample are exactly equal to the critical current J_c. At the same time, the Abrikosov vortices are fixed on the pinning centers. Local temperature fluctuations or a change of the external field, which correspond to a different value of the critical current, lead to a restructuring of the vortex system. The movement of vortices is associated with the release of energy and a corresponding increase of temperature. If the temperature increase is large enough, positive feedback causes the occurrence of vortex avalanches and significant jumps in the magnetic flux.

A common method of experimental detection of magnetic instabilities in type II superconductors is to observe the evolution of magnetization during cyclic changes in an external magnetic field H_e under constant temperature conditions of a thermostat [4–6]. In this case, the initial increase of the local temperature is induced by small changes of the magnetic flux during an increase or decrease of the external field. The magnetic flux jumps manifest themselves as a sharp decrease of the magnetization modulus on the hysteresis loops $M(H_e)$ followed by a gradual recovery. Depending on the final temperature of the sample, which was established as a result of heat generation during the movement of superconducting vortices, changes in magnetization can vary significantly, reaching a maximum value as a result of the transition to the normal state. The specific type of hysteresis loops with magnetization jumps depends on many physical parameters, such as temperature, critical current, thermal conductivity, specific heat, demagnetization factor, and a number of others.

Two main approximations were proposed in the theoretical analysis of the reaction of vortices to local overheating in the sample volume [1,7–11]. The dynamic approximation corresponds to the case when the diffusion coefficient of the magnetic flux is less than the coefficient of thermal diffusion, which leads to the propagation of heat through a system of fixed vortices and currents. The opposite case is the adiabatic heating, when the coefficient of thermal diffusion is less than the coefficient of diffusion of the magnetic flux and the thermal conduction process can be neglected.

Thermomagnetic instabilities have been studied in the most detail for bulk superconductors, both traditional and unconventional. Examples are niobium and its alloys [1,7,8,12], YBaCuO and other high-temperature superconductors [4,5], which have a low heat capacity and a sufficiently large critical current. Magnetization jumps have also been found in low-dimensional systems, for example, in thin films of Pb [13]. In many cases, numerical estimations have shown the validity of the adiabatic approximation over a wide range of field sweep rates. A more general approach,

taking into account the kinetics of heat exchange with a thermal reservoir, was proposed in Ref. [14].

Along with thin films, other low-dimensional structures are of increased interest, which are nanocomposites based on porous matrices with metal nanoparticles in the pores [15–19]. Such nanocomposites have promising technological applications in the field of superconducting nanodevices. To date, magnetic instabilities have been observed in porous Vycor glass with indium inclusions [16,17] and in porous glass with an average pore size of 7 nm with lead nanoparticles [20,21]. The magnetization jumps in porous glass with the pores filled with lead, were interpreted within the framework of the adiabatic approximation [20]. Questions about the possibility of magnetic instabilities in such nanocomposites based on other metals, their nature and patterns, as well as the validity of the same theoretical approaches used for their description in bulk type II superconductors, remain poorly studied.

This paper presents the results of an experimental study and numerical simulation of magnetic instabilities in the porous glass/Bi−Sn alloy nanocomposite.

2. Samples and experiment

Sodium borosilicate glass was used as a porous matrix, which was subjected to heat treatment for phase separation and subsequent acid leaching to obtain an interconnected pore network [22]. The pore size was controlled by nitrogen porosimetry using Quadrasorb SI analyzer manufactured by Quantachrome Instruments. The average pore size was 15 nm.

The composition of the bismuth-tin alloy was close to the eutectic point [23]: 57 wt.% Bi and 43 wt.% Sn. The alloy was introduced into the porous matrix in the molten state under pressure up to 10 kbar. The sample was cut from filled porous glass in the form of a plate with a mass of 5.78 mg. The surface of the sample was thoroughly cleaned from traces of bulk alloy.

The magnetization isotherms were measured using MPMS SQUID-VSM magnetometer manufactured by Quantum Design at several fixed temperatures in the magnetic field range from -1 to $+1$ T. Before the measurements, the samples were cooled in a zero magnetic field to the target temperature. The magnetization was then sequentially measured as the field increased to 1 T (primary magnetization), the field decreased to -1 T (secondary magnetization), and the field increased to 1 T (tertiary magnetization). The rate of change of the magnetic field was 5 G/s. Additionally, the temperature dependence of the magnetization was measured in the field of 10 G while heated from 1.8 to 10 K after cooling in a zero magnetic field (ZFC mode) and then in the subsequent cooling mode (FC) to determine the temperature of the superconducting transition in the sample.

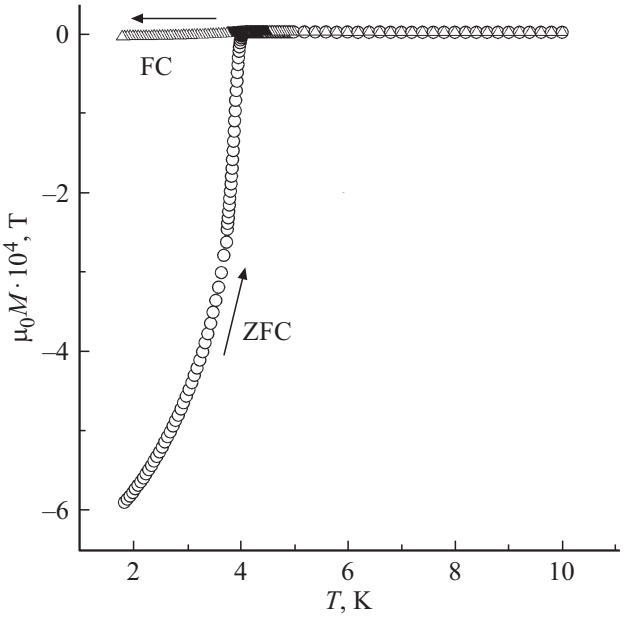

Figure 1. Temperature dependences of magnetization measured in ZFC (circles) and FC (triangles) conditions in an external field of 10 G. The arrows indicate the direction of temperature change.

3. Results

The temperature dependences of the magnetization in the field of 10 G are shown in Figure 1. The temperature of the superconducting phase transition $T_c = 4.20 \pm 0.03$ K was found as the temperature of the beginning of a noticeable deviation of the ZFC and FC curves from an almost linear course in the normal state. Only one superconducting transition is visible in the 10 G field, whereas two transitions with diamagnetism temperatures of 8.55 and 5.1 K were detected in Ref. [24] for Bi−Sn bulk alloy of the same composition. Segregates enriched in bismuth and tin with the symmetry of the corresponding bulk metals are produced in case of crystallization of the eutectic alloy Bi−Sn. It should be assumed that the observed superconducting transition in the porous glass/alloy Bi−Sn sample corresponds to the occurrence of superconductivity in segregates with the structure of tin. The temperature of transition to the superconducting state for bulk tin is 3.72 K. The shift of the transition in the studied nanocomposite, as well as in the bulk alloy, towards high temperatures may be associated with the presence of bismuth segregates. Whereas the difference in transition temperatures between nanostructured and bulk alloys is presumably attributable to the nanoconfinement effect.

The superconducting transition is significantly diffused in Figure 1. At a temperature of 1.8 K, which is equal to the lower limit of the operating range of the magnetometer used, the magnetizations measured in the ZFC and FC modes vary significantly. This corresponds to type II superconductivity in the studied sample and indicates strong pinning of superconducting vortices.

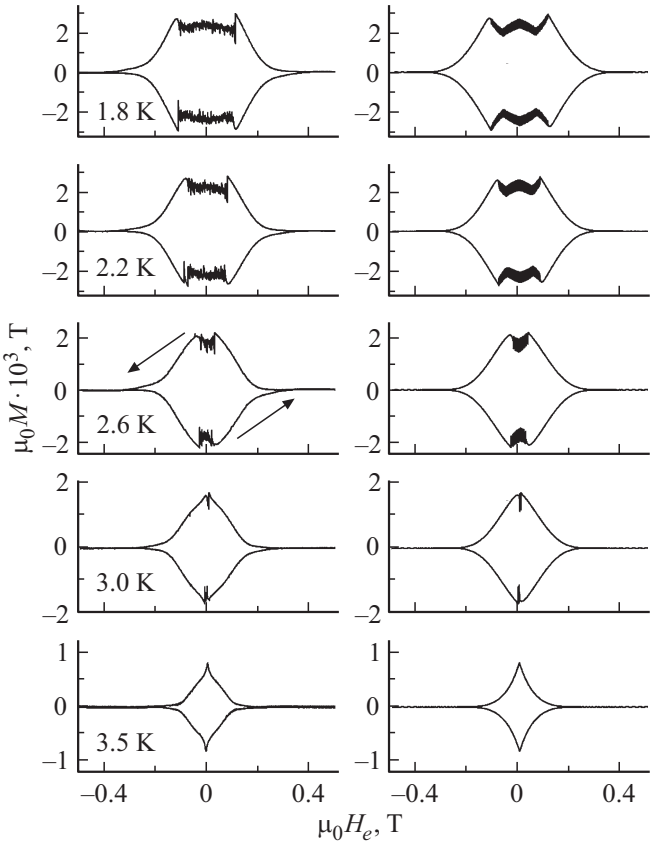

Figure 2. Experimental (on the left) magnetization isotherms acquired at the temperatures shown in the figure at the rate of change of the external magnetic field 5 G/s. The arrows indicate the direction of the change in the external field. The calculated curves for the corresponding temperatures are shown on the right.

The magnetization isotherms acquired at temperatures of 1.8, 2.2, 2.6, 3.0, and 3.5 K are shown in Figure 2. The curves of secondary and tertiary magnetization are shown. Incomplete jumps are observed on the hysteresis loops at all temperatures except 3.5 K. The peculiarity of these jumps is that they occur only in the central part of the hysteresis loops and at very short intervals of changes in the external field. This result indicates a complex dependence of the critical current on the magnitude of the magnetic field.

4. Discussion

The model described in Refs. [4,6,7,9,20,25] is used in this study for numerical simulation of magnetization isotherms, with modified field dependence of the critical current and the dynamics of temperature changes after a magnetic flux jump.

Let us consider a plate of type II superconductor with a thickness $2L$, oriented along the axis x ($x = 0$ corresponds to the middle of the plate) and infinite in the directions y and z. A uniform external magnetic field is applied parallel to the plate surface in the direction z. The magnetic field H in the plate is also parallel to the axis z and depends only on x. For this geometry, currents, if they are not equal to zero, flow along the axis y. It is assumed that the plate is in the critical state, so the current density J inside the plate can be written as:

$$J(x, T, H) = s(x)J_c(T, H), \tag{1}$$

where T is the temperature, H is the magnetic field in the plate, $s(x) = \pm 1$ in areas where the magnetic field penetrates, and $s(x) = 0$ where there is no field. J_c indicates the absolute value of the critical current density. It is assumed that J_c depends linearly on temperature at temperatures below critical:

$$J_c(T, H) = J_0\left(1 - \frac{T}{T_c}\right)\theta(T_c - T)g(H), \tag{2}$$

where θ is the Heaviside theta function, T_c is the critical temperature, J_0 is a constant that is a parameter of the model. The factor $g(H)$ describes the dependence of the critical current on the field. Various functions are used as $g(H)$, ranging from the simplest Bean model [15] with $g(H) \equiv 1$ to rather complex dependencies, such as the peak effect model [25], in which

$$g(H) = \frac{1}{(1 + |H|/H_0)} + \frac{K(|H|/H_p)}{\left(1 + (1 - |H|/H_p)^2\right)}, \tag{3}$$

where H_0, H_p and K are numerical parameters. The previously applied functions did not allow achieving a good correspondence between the results of numerical modeling and experiment for the nanocomposite that we studied, therefore, we introduced a new generalized power-law model in this work:

$$g(H) = \left(1 - \frac{|H|}{H_0}\right)^{\left[K_1 \frac{|H|}{H_0} + K_2\left(1 - \frac{|H|}{H_0}\right)\right]} \theta(H_0 - |H|). \tag{4}$$

Here K_1, K_2, H_0 are fitting parameters. It should be noted that the usual (with fixed exponent) power model

$$g(H) = \left(1 - \frac{|H|}{H_0}\right)^K \theta(H_0 - |H|) \tag{5}$$

was discussed earlier in Ref. [6]. In the generalized model, the exponent linearly varies with the field from K_2 to K_1 as the field increases from zero to H_0, which in this model plays the role of the second critical field. This model best matched the shape of the hysteresis loops.

The magnetic field profile in the sample at temperature T is determined from the Maxwell equation, which gives the following critical state equation for this geometry:

$$\frac{\partial H}{\partial x} = -s(x)J_c(T, H). \tag{6}$$

The conditions $H(\pm L) = H_e$ must be met on the surface of the plate, where H_e is the applied external field. It is obvious

that $H(x) = H(-x)$ for symmetry reasons. It should be noted that in the general case, a continuously differentiable solution to such a boundary value problem may not exist. Therefore, instead of solving the boundary value problem in the interval $[-L, L]$, we consider the Cauchy problem in the interval $[-L, 0]$ with the initial condition $H(-L) = H_e$ and continue the solution over the upper half of the plate based on symmetry.

The magnetization can be calculated as follows:

$$M = \frac{1}{L}\int_{-L}^{0} H dx - H_e. \tag{7}$$

A magnetic flux jump occurs when the instability condition is met [9]:

$$\Delta H_s > \Delta H_e, \tag{8}$$

where ΔH_e is a slight increase in the applied external field, and ΔH_s is a weakening of the shielding ability of the sample as a result of a local temperature increase caused by the restructuring of the superconducting vortex system.

It should be noted for calculating ΔH_s that an increase of the magnetic field by ΔH_e leads to the emergence of an electric field depending on the coordinate x and time t $E(x, t)$, directed along the y axis (Faraday's law):

$$E(x, t) = \mu_0 \int_{x}^{x_0} \frac{dH(x_1, t)}{dt}\, dx_1, \tag{9}$$

where the coordinate $x_0 \le 0$ corresponds to the plane up to which the field penetrates into the sample ($x_0 = 0$ in the case of full penetration). This leads to the release of heat, the amount of which per unit volume in the vicinity of x for a short time Δt is equal to:

$$\Delta Q(x) = J(x)\int_{0}^{\Delta t} E(x, t)dt$$

$$= \mu_0 s(x) J_c\big(T, H(x)\big)\int_{x}^{x_0} \Delta H(x_1)dx_1. \tag{10}$$

When deriving the last expression, equation (9) was taken into account. $\Delta H(x_1)$ in (10) is a (small) field change at $x = x_1$ during time Δt. The release of heat leads to a local increase of temperature:

$$\Delta T(x) = \frac{\Delta Q(x)}{C_V}, \tag{11}$$

where C_V is the heat capacity per unit volume of the nanocomposite. An increase of temperature, in turn, causes a decrease of the critical current:

$$\Delta J_c(x) = \frac{\partial J_c}{\partial T}\Delta T(x) \tag{12}$$

and a corresponding change of shielding capacity

$$\Delta H_s = -\int_{-L}^{x_0} s(x)\Delta J_c(x)dx. \tag{13}$$

Taking into account the results obtained and the equality of $s^2(x) = 1$ for $-L \le x \le x_0$, we write the instability condition as follows:

$$\frac{\Delta H_s}{\Delta H_e} = -\frac{\mu_0}{C_V}$$

$$\times \int_{-L}^{x_0}\left[\frac{\partial J_c\big(T, H(x)\big)}{\partial T} J_c\big(T, H(x)\big)\int_{x}^{x_0}\frac{\Delta H(x_1)}{\Delta H_e}\, dx_1\right]dx > 1. \tag{14}$$

Considering the field H as a function of the external applied field and letting ΔH_e to zero, the ratio $\frac{\Delta H(x)}{\Delta H_e}$ can be replaced by a partial derivative

$$\frac{\partial H(x, H_e, T)}{\partial H_e} \equiv \alpha(x, H_e, T). \tag{15}$$

The function $\alpha(x, H_e, T)$, considered as a function of the variable x for fixed H_e and T, satisfies the Cauchy problem obtained by differentiating the critical state equation (6) with respect to the external field and the boundary condition:

$$\begin{cases} \dfrac{\partial \alpha}{\partial x} = -s(x)\dfrac{\partial J_c}{\partial H}\alpha, \\ \alpha\big|_{x=-L} = 1. \end{cases} \tag{16}$$

The problem (16) is solved numerically, taking into account the current density and field distributions known at each step. The resulting solution allows finding the left side of equation (14) and verify the fulfillment of inequality (8).

Usually, when performing calculations within the framework of the adiabatic approximation, it is assumed that the magnetization jump is associated with an increase of the sample temperature above the thermostat temperature, as a result of which a new current and field profile is established. Immediately after the jump, the sample temperature returns to the initial value, and the fixed profile „freezes" [4]. The process of relaxation of the sample temperature to the thermostat temperature is thus not considered and is assumed almost instantaneous. However, within the framework of this approach, we were unable to achieve a satisfactory agreement between the calculated and experimental hysteresis loops. The analysis showed that a good simulation result can be achieved assuming a finite rate of thermal equilibrium between the sample and the thermostat. Let us assume that the sample temperature increases by a value ΔT_j (a model parameter) during a jump, then rapidly decreases by a value ΔT_d (smaller than ΔT_j and also a fitting parameter), after which it relaxes exponentially with a relaxation time τ until the next magnetization jump occurs:

$$\frac{d}{dt}(T_p - T_0) = -(T_p - T_0)/\tau. \tag{19}$$

The temperature $T_p(t)$ is used for calculating the field and current profiles outside of magnetization jumps. The increments of the external field and the corresponding time intervals are related by the rate of change of the external field. When the external field is cycled, the current and field profiles gradually change, starting from the plate surface. In this case, $s(x) \geq 0$ $(s(x) \leq 0)$ for an increasing (decreasing) external field.

The hysteresis loops obtained on the basis of the described model are shown in Figure 2. As can be seen, the theoretical loops are in good agreement with the experimental results.

Figures 3–5 show the temperature dependences of the fitting parameters used in the calculation.

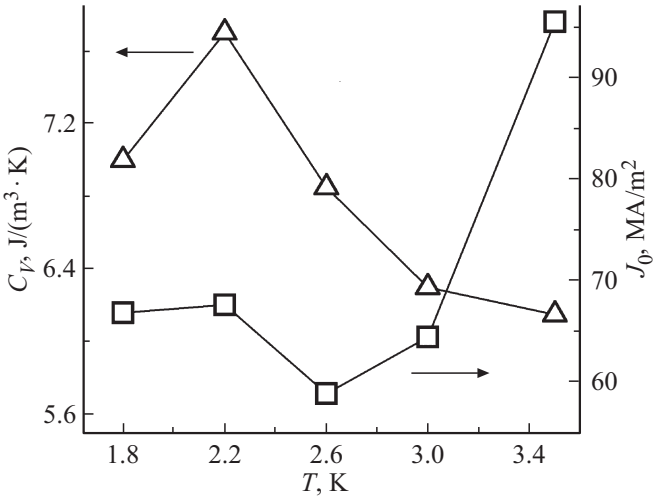

Figure 3. The dependences of the fitting parameters C_V (triangles) and J_0 (squares) in the equations (11) and (2), respectively, on temperature.

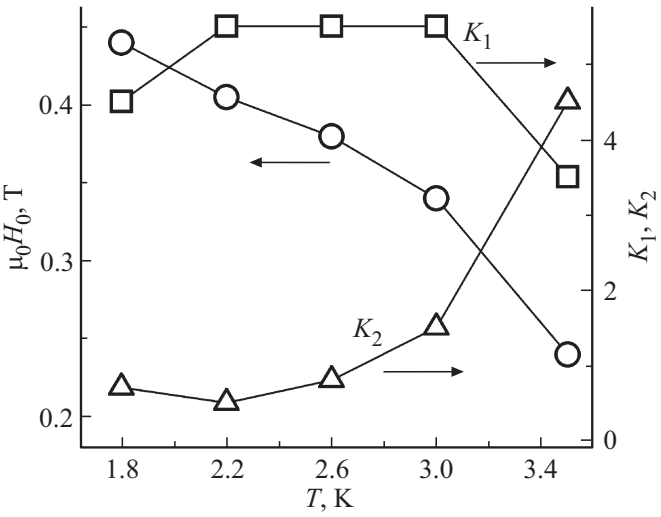

Figure 4. Temperature dependence of the fitting parameters H_0 (circles), K_1 (squares) and K_2 (triangles) in the equation (4).

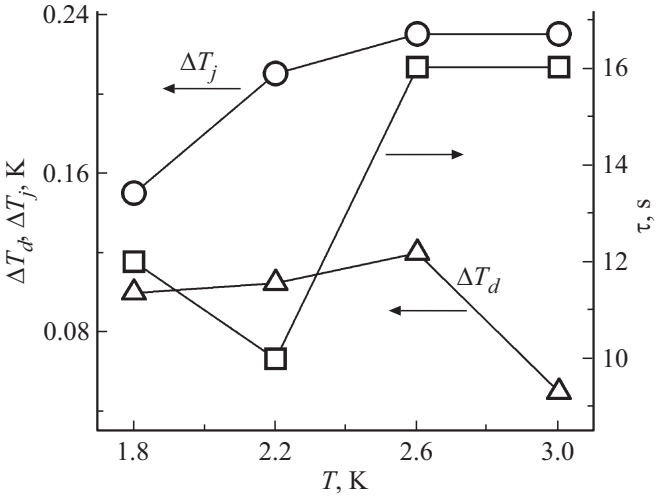

Figure 5. Temperature dependences of the fitting parameters ΔT_j (circles) and ΔT_d (triangles), equal to an increase of temperature in case of a magnetization jump and a decrease of temperature immediately after the jump, respectively, and the relaxation time τ in the equation (19).

5. Conclusion

It is shown that the temperature of transition to the superconducting state for a nanocomposite based on the porous glass with an average pore size of 15 nm filled with Bi–Sn alloy of the eutectic composition is 4.2 K. The temperature and field dependences of the magnetization indicate that the nanocomposite belongs to dirty type II superconductors. The instabilities observed on the magnetization isotherms can be treated using an adiabatic approach with a complicated relationship of the critical current with the magnetic field and taking into account the relaxation of the sample temperature after a magnetic flux jump.

Funding

The study was conducted within the framework of the St. Petersburg State University initiative project INI_2024. The measurements were performed using the equipment of the Resource Center of „Centre for Diagnostics of Functional Materials for Medicine, Pharmacology and Nanoelectronics“ of Saint Petersburg State University Research Park.

Conflict of interest

The authors declare that they have no conflict of interest.

References

[1] R.G. Mints, A.L. Rakhmanov. Rev. Mod. Phys. **53**, 551 (1981).
[2] E. Altshuler, T.H. Johansen. Rev. Mod. Phys. **76**, 471 (2004).

[3] Ch. Huang, Z. Song, Sh. Wang, H. Chen, F. Wang. Supercond. Sci. Technol. **36**, 015008 (2023).
[4] K.-H. Müller, C. Andrikidis. Phys. Rev. B **49**, 1294 (1994).
[5] A. Gerber, J.N. Li, Z. Tarnawski, J.J.M. Franse, A.A. Menovsky. Phys. Rev. B **47**, 6047 (1993).
[6] C. Romero-Salazar, F. Morales, R. Escudero, A. Durán, O.A. Hernández-Flores. Phys. Rev. B **76**, 104521 (2007).
[7] Y.B. Kim, C.F. Hempstead, A.R. Strand. Phys. Rev. **129**, 528 (1963).
[8] L. Wipf. Phys. Rev. **161**, 404 (1967).
[9] P.S. Swartz, C.P. Bean,. J. Appl. Phys. **39**, 4991 (1968).
[10] R. Hancox. Phys. Lett. **16**, 208 (1965).
[11] D. Livingston. Appl. Phys. Lett. **8**, 319 (1966).
[12] M.R. Wertheimer, J. le G. Gilchrist. J. Phys. Chem. Sol. **28**, 2509 (1967).
[13] A.V. Silhanek, S. Raedts, V.V. Moshchalkov. Phys. Rev. B **70**, 144504 (2004).
[14] Y.-H. Zhou, X. Yang. Phys. Rev. B **74**, 054507 (2006).
[15] C.P. Bean. Rev. Mod. Phys. **36**, 31 (1964).
[16] J.H.P. Watson. Phys. Rev. **2**, 1282 (1970).
[17] F. Dong, M.J. Graf, T.E. Huber, C.I. Huber. Solid State Commun. **101**, 929 (1997).
[18] E.V. Charnaya, C. Tien, K.J. Lin, C.S. Wur, Yu.A. Kumzerov. Phys. Rev. B **58**, 467 (1998).
[19] C. Tien, C.S. Wur, K.J. Lin, E.V. Charnaya, Yu.A. Kumzerov. Phys. Rev. B **61**, 14833 (2000).
[20] C. Tien, A.L. Pirozerskii, E.V. Charnaya, D.Y. Xing, Y.S. Ciou, M.K. Lee, Yu.A. Kumzerov. J. Appl. Phys. **109**, 053905 (2011).
[21] C. Tien, E.V. Charnaya, D.Y. Xing, A.L. Pirozerskii, Yu.A. Kumzerov, Y.S. Ciou, M.K. Lee. Phys. Rev. B **83**, 014502 (2011).
[22] Two-phase glasses: structure, properties, application. Ed. by B.G. Varshal. L.: Nauka, 1991, 275 p. (in Russian).
[23] M.H. Braga, J. Vizdal, A. Kroupa, J. Ferreira, D. Soares, L.F. Malheiros. Calphad **31**, 468 (2007).
[24] M.V. Likholetova, E.V. Charnaya, E.V. Shevchenko, Yu.A. Kumzerov. FTT **63**, 208 (2021). (in Russian).
[25] V.V. Chabanenko, A.I. D'yachenko, M.V. Zalutskii, V.F. Rusakov, H. Szymczak, S. Piechota, A. Nabialek. J. Appl. Phys. **88**, 5875 (2000).

Translated by A.Akhtyamov